Bortolan Neto, Luiz; Kotousov, Andrei Georgievich
Residual opening of hydraulic fractures filled with compressible proppant
International Journal of Rock Mechanics and Mining Sciences, 2013; 61:223-230

DOI: 10.1016/j.ijrmms.2013.02.012

Residual Opening of Hydraulic Fractures Filled with Compressible Proppant

Luiz Bortolan Neto and Andrei Kotousov

School of Mechanical Engineering

The University of Adelaide, Adelaide SA 5005 Australia

luiz.bortolanneto@adelaide.edu.au, andrei.kotousov@adelaide.edu.au

Abstract

In hydraulic stimulations, which are widely utilised in petroleum and gas industries to enhance the permeability of reservoirs and improve the productivity of wells, an injection of proppant (or small particles) is normally needed to avoid the closure of the opened artificial and natural fractures under confining stresses. The residual openings of these fractures determine the efficiency and, in general, success of the hydraulic stimulations. Despite the vast number of papers devoted to fluid driven fractures and hydraulic stimulation procedures, there is not much research focusing on the residual fracture profiles. This problem is characterised by a strong non-linearity and represents a challenge for numerical modelling. In this paper a simple semi-analytical method for calculating the residual openings of fractures partially filled with proppant is developed. It is based on the Distributed Dislocation Technique and Terzaghi's classical consolidation model. One of the results of simulations indicates that the proppant distribution and its mechanical properties have a significant influence on the residual fracture profiles.

Keywords: Hydraulic well stimulation, Well productivity, Residual fracture opening, Distributed Dislocation technique, Terzaghi's consolidation model

1 Introduction

Hydraulic stimulations are very common in oil and gas industries to enhance the hydrocarbon recovery of geological reservoirs. These stimulations normally include a fracture initiation stage with the following propagation and opening of the artificial or natural fractures by a pressurised fluid. On a later stage, granular particles (proppant) are injected with the fracturing fluid to avoid closure of the opened fractures during the production stage. These fractures filled with proppant can significantly enhance the permeability of reservoirs and improve the productivity of wells.

Over the past fifty years several approaches have been developed to model the stress state, fracture initiation conditions and profile of fractures driven by various pressurised fluids. These approaches are widely used in the design of hydraulic stimulation procedures and comprehensive reviews can be found, for example, in text books and review articles [1–4]. Nevertheless, not much attention has been given to the residual openings, which take place after the hydraulic pressure is released. Meanwhile, these residual openings are directly linked to the fracture conductivity [5] and, therefore, represent the main outcome of well stimulations. The residual openings significantly affect the productivity of reservoirs and, finally, determine the success of the stimulation procedures.

Among other parameters, such as the level of the opening pressure, magnitude of the confining stresses, length of the fracture and mechanical properties of the proppant and surrounding rock/medium, the residual openings also depend on the proppant distribution inside the fracture. In a general case (see Figure 1 as an illustration only), a hydraulic fracture can be partially filled with proppant leading to the reduction of the fracture opening profile in comparison with the case when the proppant occupies the whole space within the fracture.

The pioneering study by Kern et al. [6] first investigated the transport of sand in vertical hydraulic fractures. It was observed a significant settling of proppant near the wellbore area. This normally leads to the build up of a mound of settled sand on the bottom face of a vertical fracture, as illustrated in Figure 1. The proppant build up develops and grows until the fluid flow velocity is relatively high to provide the vertical movement to the injected particles.

After Kern et al. [6], a number of other experimental works on proppant transport were conducted for horizontal fractures; see for example [7,8]. Numerical and analytical studies on proppant settling were reviewed in [9]. All these works, including [10–15] and, more recently, [16] have confirmed the rise of the profile of the settled proppant in the vicinity of the wellbore. The outcomes of the above theoretical studies were validated with the use of experimental approaches utilising the sonic borehole televiewer, the Formation MicroScanner tool, impression packers, down-hole closed circuit television, and mapping techniques (see [17] for a comprehensive overview).

In the absence of other fracture opening mechanisms (such as the shear slip opening [18–20]), once the hydraulic pressure is removed, the fracture surfaces will be subjected to confining stresses leading to the closure of the opened fractures developed during the initial stages of hydraulic stimulation. Therefore, the distribution of the proppant along the fracture is expected to significantly influence the residual profile of the fracture along with the compressibility of the proppant and mechanical properties of the surrounding rock.

In this paper we develop a simplified semi-analytical method for calculating the residual opening of fractures partially filled with proppant, which takes into account the non-linear compressibility of the proppant. This method is based on the Distributed Dislocation Technique (DDT) [21,22], that is applied to simulate the mechanics of cracks. The response of the proppant to the applied stress is modelled by Terzaghi's classic consolidation model [23]. The choice of the Terzaghi’s model is justified by its simplicity and wide use; however the developed method can easily accommodate other models of mechanical behaviour of proppant, such as models of low consolidated media available in the literature (e.g. [24,25]). Further, we also utilise an iterative procedure to obtain a solution to the strongly non-linear problem of determining the fracture closure. It was found surprising that the same method can be applied to a totally different area of composite patching repair widely used in aircraft industry to restore the strength of damaged structures. This is due to the similarity of the mathematical formulations of both problems. Thus, the previous works on composite patching provided a benchmark solution against which the present method was validated.

In the beginning of the paper we will formulate the mechanical model, which will be followed by a mathematical formulation of the closure model. After that, a method for calculating the residual opening will be presented and the validation of the model and its comparison to available benchmark solutions will follow. The paper will be concluded with a discussion of the obtained results and possible future work.

2 Mechanical Model

Consider a hydraulic fracture of half length a with an internal fluid pressure p, as shown in Figure 2a. In the absence of the hydraulic pressure, p, the confining stresses, σ^{∞}, will lead to a reduction of the original fracture opening, as illustrated in Figure 2b. This change in the fracture opening depends on the proppant mechanical response to the compression loading as well as on the distribution of the proppant inside the fracture.

The closure of a hydraulic fracture is a very complex phenomenon due to the coupling of many non-linear physical processes [26]. In order to develop a mathematical model of this phenomenon we have to adopt some simplifications and assumptions, which are typical for analytical and numerical studies. These simplifications and assumptions will be briefly introduced and discussed next.

In the beginning we will reduce the number of dimensions of this complex three-dimensional problem. In the following we will consider a two-dimensional (2D) centred fracture in an infinite elastic medium placed along the line segment $|x| \le a$, $y = 0$. The medium is assumed to be impermeable, isotropic, homogeneous, and linearly elastic with Young's modulus E and Poisson's ratio ν. The fracture is subjected to a remote, normal, uniform compressive stress, σ^∞, such that

$$\sigma_{yy}\left(x^2 + y^2 \to \infty\right) = \sigma^\infty . \tag{1}$$

A fluid pressure, p, is acting inside the fracture. The induced pressure by the fluid is assumed to be uniform over the total length of the crack. Generally, when the medium is permeable and fracture openings are relatively small, the pressure may change significantly along the fracture length. The fluid flow in narrow openings is normally described by equations of lubrication theory [27–29], namely local and global continuity equations and the Poiseuille law. This theory predicts that the fluid pressure behaves at fracture tips as $p \propto \ln(x)$ for the case of infinite fracture toughness and as $p \propto -x^{-1/3}$ in the case of zero fracture toughness [30]. This extremely complicates the matter because a fluid cannot sustain infinite suction (negative pressure) and, therefore, further assumptions have to be introduced to resolve this issue. Nonetheless, in the present work, as well as in a number of other studies (e.g. [31–33]), it is assumed that this zone is very small and does not affect significantly the stress state surrounding the fracture neither the fracture conditions. Hence, according to the linear fracture mechanics, a constant fluid pressure, $p > 0$, inside the fracture and remote confining stresses, $\sigma^\infty < 0$, will lead to an initial fracture opening, $\delta_0(x)$, if $\sigma^\infty + p > 0$, as illustrated in Figure 2a. The fracture profile is then given by the classical equation

$$\delta_0(x) = 4\frac{\sigma^\infty + p}{\overline{E}}\sqrt{a^2 - x^2}\,; \tag{2}$$

$\overline{E}$ being the reduced or generalised Young's modulus defined as: $\overline{E} = E$, for plane stress, and $\overline{E} = E/\left(1-\nu^2\right)$, for plane strain conditions. The latter is more appropriate for large fractures in geological reservoirs [1–4]. The stress intensity factor associated with the initial opening can be calculated as

$$K_0 = \left(\sigma^{\infty} + p\right)\sqrt{\pi a}\,. \tag{3}$$

Following the removal of the fluid pressure inside the fracture, the proppant distributed inside the fracture will prevent the fracture from full closure (as illustrated in Figure 2b). The residual opening $\delta(x)$, being $\delta(x) = \Delta\delta(x) + \delta_0(x)$, will be obtained from the governing equations for the problem under consideration. These equations will be introduced in the next section.

The mechanical model discussed above leads to the following set of boundary conditions of the problem, which have to be satisfied by the solution:

$$\sigma_{yy}(x, y) = \sigma^{\infty}\,,\ x^2 + y^2 \to \infty\,; \tag{4a}$$

and, at $y = 0$,

$$\sigma_{yy}(x, y) = \sigma^{\infty} - \sigma'_n(x),\ |x| \le b\,, \tag{4b}$$

$$\delta(x) = 0\,,\ |x| > a\,; \tag{4c}$$

where b is the settled proppants length and σ'_n is the normal effective stress due to proppant. The latter can depend both on the fracture residual opening and mechanical properties (response) of the proppant.

The settled proppants length depends on the transport, settling and concentration of proppants after the proppant injection phase is complete [3]. However, the modelling of these very important phenomena is beyond the scope of the present paper.

It is also assumed that the pressure inside the fracture at the production stage are negligible in comparison with the confining stresses, and, therefore, can be disregarded in the calculation of the residual opening and stresses along the fracture. Next, the governing equations will be presented followed by a mathematical model describing the proppant mechanical response.

3 Mathematical Model

There are a number of mathematical approaches that can be employed to solve the problem presented above, such as the Distributed Dislocation Technique (DDT) [21,22], formulations based on integral equations with hypersingular kernels [34–37] and numerical techniques based on the Boundary Integral Equation Method [38,39]. In this work we applied the DDT as it has proved to be a very efficient method for solving Fracture Mechanics problems.

Therefore, from the boundary conditions presented above (see Eq. (4)) along with the aid of the DDT it is possible to obtain the governing equation for the problem. This equation is derived below for an arbitrary model of the proppant mechanical response. Later, in order to conduct an analysis of the residual openings, we will formulate a specific mechanical model for the proppant physical behaviour, which utilises Karl Terzaghi's classical consolidation model for cohesionless particles (e.g. sand). The use of such model is justified as sand is often utilised as proppant in hydraulic stimulations [8].

3.1 Governing Equations

In their classic work Bilby and Eshelby [40] postulated that the perturbation of the uniform stress field in a body owing to the presence of a fracture may be deemed due to the existence of a distribution of dislocations along $|x| \le a$, $y = 0$. Therefore, for the formulated boundary conditions of the problem under consideration, the stresses along the fracture opening can be found from the dislocation density $\rho(x)$ as [41]:

$$\sigma_{xx}(x) = \frac{\overline{E}}{4\pi} \int_{-a}^{a} \frac{\rho(\xi)}{x-\xi} d\xi \tag{5}$$

and

$$\sigma_{yy}(x) = \frac{\overline{E}}{4\pi} \int_{-a}^{a} \frac{\rho(\xi)}{x-\xi} d\xi + \sigma^{\infty} . \tag{6}$$

The out-of-plane stress component being a consequence of the accepted plane strain assumption is then given by

$$\sigma_{zz} = \nu\left(\sigma_{xx} + \sigma_{yy}\right). \tag{7}$$

The dislocation density is not known a priori and it has to be found from the solution of the problem. The dislocation density $\rho(x)$ must be found in such way that it fulfils the following integral equation:

$$\frac{\overline{E}}{4\pi} \int_{-a}^{a} \frac{\rho(\xi)}{x-\xi} d\xi = -\sigma^{\infty} + \sigma'_{n}(x),\ |x| \le a . \tag{8}$$

An additional requirement, which has to be satisfied with the dislocation representation of the fracture, is that the net content of a fracture should vanish, giving rise to the following additional single-valued condition for the dislocation density function [21]:

$$\int_{-a}^{a} \rho(\xi) d\xi = 0. \tag{9}$$

The dislocation density $\rho(x)$ and the fracture residual opening $\delta(x)$ are related to each other by the following equation [22]:

$$\delta(x) = -\int_{-a}^{x} \rho(\xi) d\xi \, . \tag{10}$$

The exact solution of the singular integral equation (8) with the additional condition (9) introduced above is not straightforward and requires inversion of the non-linear integral equation with Cauchy kernel. This can be achieved with a numerical procedure based, for example, on Gauss-Chebyshev quadrature method, which will be discussed in Section 4.

3.2 Proppant response

One of the most important properties of non-consolidated particles is its compressibility. One of the first models describing its mechanical response was developed by Karl Terzaghi and since then several other mathematical models were suggested by many researchers aiming to simulate the compressive behaviour of cohesionless particles. Pestana and Whittle [42] provided an overview of such mechanical models from which it becomes evident that their accuracy over Terzaghi's original model comes at the expense of additional unknown parameters or coefficients, which need to be obtained experimentally. This, however, significantly complicates the modelling without providing an explicit superiority over the original work by Terzaghi. Therefore, in the current study we adopt the classical Terzaghi model to estimate the proppant response due to compressive loading.

In the one-dimensional Terzaghi's consolidation model both pore water and particles are assumed to be incompressible. Thus, only changes in the volume of voids can be directly linked to the deformations [23]. The model also relies on the non-consolidated particles compressive behaviour. This behaviour is generally non-linear and geotechnical engineers usually described it by using the index property C_c (which is a function of the void ratio e and of the normal effective stress σ_n') in conjunction with qualitative descriptions of stress levels, such as presented by Vesic and Clough [42,43]. The settlement deformation $\Delta\delta(x)$ can be written as [23]

$$\Delta\delta(x) = C\delta_0(x)\ln(\sigma'_n(x)/\sigma'_{n0}); \tag{11}$$

with C being the particles assembly compressibility, σ'_{n0} the initial normal effective stress acting on the particles, and $\delta_0(x)$ is the fracture initial opening given by Eq. (2). As mentioned above, C relates to the compression index C_c and to the initial void ratio e_0 by the following equation [44]:

$$C = C_c/(1+e_0). \tag{12}$$

Coduto [44] suggested a classification of the particle assembly compressibility (see Table 1) based on the C value.

With the introduction of the identity

$$\Delta\delta(x) = \delta_0(x) - \delta(x) \tag{13}$$

and after some algebraic manipulation with Eq. (11), the normal effective stress acting on the proppants, $\sigma'_n(x)$, can be rewritten as

$$\sigma'_n(x) = \exp(\lambda(x)/C)\sigma'_{n0}, \tag{14}$$

where the non-dimensional parameter $\lambda(x)$ is given by

$$\lambda(x) = (\delta_0(x) - \delta(x))/\delta_0(x). \tag{15}$$

If the condition $\delta(x) \propto \delta_0(x)$ holds, the parameter $\lambda(x)$ is then reduced to a constant. For this case, $\sigma'_n(x)$ will also be a constant.

Although Eq. (14) is not applicable for low stress conditions (i.e. when the proppant assembly has an unstable behaviour) it works well for conditions of moderate to high stresses (i.e. after the proppant packing has acquired a stable condition).

The mechanical response of the proppant presented above is just one of several models available in the literature [42]. However, there is no conceptual limitation that prevents the utilisation of more complicated or more comprehensive models in the solution procedure, which will be presented next.

4 Solution Procedure

The governing singular integral equation, Eq. (8), has to be solved for the unknown density of dislocations, $\rho(x)$. As it was pointed out above, an exact analytical solution is not possible with a strong non-linear mechanical response of the proppant. Furthermore, the singular term, $(x-\xi)^{-1}$, known as the Cauchy kernel of the integral, requires special integral procedures for obtaining a viable solution. One of the effective solution approaches is based on the Gauss-Chebyshev quadrature method, which will be implemented in the current study, and it will be discussed next.

4.1 Numerical formulation

The first step in the numerical solution method is to introduce a length normalisation to transform the interval $[-a,+a]$ to $[-1,+1]$ as follows:

$$s = \xi / a \tag{16a}$$

and

$$t = x / a \,. \tag{16b}$$

At the tips of the cracks the dislocation density $\rho(s)$ tends to infinity as an inverse square root while at the same time $|s|$ approaches the unity. Thus, the dislocation density can be represented as a product of the fundamental solution, $1/\sqrt{1-s^2}$, and an unknown regular function, $\phi(s)$, such that [22,41,45,46]

$$\rho(s) = \phi(s) / \sqrt{1-s^2} \,. \tag{17}$$

Therefore, with the application of the normalisations as introduced in Eq. (16) along with the Gauss-Chebyshev quadrature for N sampling points, the governing equations (8) – (10) can be transformed to a system of non-linear algebraic equations as

$$\frac{\overline{E}}{4N} \sum_{i=1}^{N} \frac{\phi(s_i)}{t_j - s_i} = -\sigma^{\infty} + \sigma_n'(t_j), \tag{18}$$

$$\frac{\pi a}{N} \sum_{i=1}^{N} \phi(s_i) = 0 \,, \tag{19}$$

and

$$\delta(t_j) = \frac{\pi a}{N} \sum_{i=1}^{j} \phi(s_i); \tag{20}$$

with $i = 1,2 \ldots N$, $j = 1,2 \ldots N-1$ and s_i, t_j being the discrete integration and collocation points of the Gauss-Chebyshev method given, respectively, by

$$s_i = \cos\left(\pi \frac{2i-1}{2N}\right) \tag{21a}$$

and

$$t_j = \cos\left(\pi \frac{j}{N}\right). \tag{21a}$$

Additionally, following Eq. (14), the normal effective stress acting on the proppant at a position t_j, $\sigma'_n(t_j)$, can be written as

$$\sigma'_n(t_j) = \exp(\lambda(t_j)/C)\sigma'_{n0}. \tag{22}$$

Substituting Eq. (20) into Eq. (15), the non-dimensional parameter, $\lambda(t_j) = \lambda_j$, becomes

$$\lambda_j = 1 - \frac{\pi a}{N\delta_0(t_j)} \sum_{i=1}^{j} \phi(s_i). \tag{23}$$

The numerical equations detailed above represent a system of non-linear algebraic equations, which can be solved computationally using, for example, an iterative procedure, which will be described next.

4.2 Computational formulation

The non-linear numerical equations presented above can be rewritten in a matrix or array form and solved computationally via the well known Newton-Raphson iterative scheme. In this scheme, the problem solution is obtained by truncating the Taylor expansion of a function at the lth iteration, $f(\phi^{(l)})$, after the linear term [47]. In matrix notation the Newton-Raphson solution of the dislocation vector $\boldsymbol{\varphi}$ assumes the form

$$\boldsymbol{\varphi}^{(l+1)} = \boldsymbol{\varphi}^{l} - \mathbf{J}^{-1(l)}\mathbf{S}^{(l)} \tag{24}$$

for the following set of arrays:

$$\boldsymbol{\varphi}^{T} = \{\varphi_1 \quad \varphi_2 \quad \cdots \quad \varphi_N\}, \tag{25}$$

$$\mathbf{J} = \begin{bmatrix} J_{1,1} & J_{1,2} & \cdots & J_{1,N} \\ J_{2,1} & J_{2,2} & \cdots & J_{2,N} \\ \vdots & \vdots & \ddots & \vdots \\ J_{N,1} & J_{N,2} & \cdots & J_{N,N} \end{bmatrix} = \begin{bmatrix} \partial f(\varphi_1)/\partial\varphi_1 & \partial f(\varphi_1)/\partial\varphi_2 & \cdots & \partial f(\varphi_1)/\partial\varphi_N \\ \partial f(\varphi_2)/\partial\varphi_1 & \partial f(\varphi_2)/\partial\varphi_2 & \cdots & \partial f(\varphi_2)/\partial\varphi_N \\ \vdots & \vdots & \ddots & \vdots \\ \partial f(\varphi_N)/\partial\varphi_1 & \partial f(\varphi_N)/\partial\varphi_2 & \cdots & \partial f(\varphi_N)/\partial\varphi_N \end{bmatrix}, \tag{26}$$

and

$$\mathbf{S}^T = \{S_1 \quad S_2 \quad \cdots \quad S_N\}. \tag{27}$$

The elements of the dislocation vector, φ_i, represent the value of the unknown function ϕ at the point s_i $(\varphi_i = \phi(s_i))$. From Eqs. (18) and (19) it is possible to obtain both the Jacobian matrix, $\mathbf{J}$, and the confining stress vector, $\mathbf{S}$, components, which are given by

$$J_{j,i} = \frac{\overline{E}}{4N(t_j - s_i)} + \mathrm{H}(j-i)\frac{\pi a}{NC}\frac{\sigma'_n(t_j)}{\delta_0(t_j)}, \tag{28a}$$

$$J_{N,i} = a\pi/N, \tag{28b}$$

$$S_j = \sigma^\infty, \tag{29a}$$

$$S_N = 0; \tag{29b}$$

with $i = 1,2\ldots N$, $j = 1,2\ldots N-1$, $\sigma'_n(t_j)$ given by Eq. (22), and $\mathrm{H}(j-i)$ being the well known Heaviside step function.

Rearranging Eq. (24) yields the following $N \times N$ system of non-linear equations at the l th iteration:

$$\mathbf{J}^{(l-1)}\boldsymbol{\Delta\varphi}^{(l)} = \mathbf{S}, \tag{30}$$

with the improved dislocation solution being

$$\boldsymbol{\varphi}^{(l)} = \boldsymbol{\varphi}^{(l-1)} + \boldsymbol{\Delta\varphi}^{(l)}. \tag{31}$$

The system given by Eq. (30) is solved for $l = 1, 2, 3\ldots$ by the utilisation of standard methods (e.g. Gaussian elimination) until $\boldsymbol{\Delta\varphi}^{(l)}$ is sufficiently small.

To verify if the solution has reached an acceptable value, an appropriate convergence criterion must be employed. One of such has been discussed in [48] and it simply consists of verifying at each iteration step the following relationship:

$$\frac{\left\|\boldsymbol{\Delta\varphi}^{(l)}\right\|_2}{\left\|\boldsymbol{\varphi}^{(l)}\right\|_2} \le \varepsilon, \tag{32}$$

where ε is the dislocation convergence tolerance.

4.3 Analysis of Stresses

Once an appropriate solution for the unknown function $\phi(s_i)$ is obtained it is then possible to determine the stresses along the fracture as well as the stress intensity factors.

An asymptotic analysis of the crack tip opening displacement (CTOD) can be performed for the singular points (tips of the crack) providing the following expression for the stress intensity factor [21]:

$$K = \frac{4}{\overline{E}}\sqrt{\pi a}\,\phi(\pm 1). \tag{33}$$

Equation (20) allows the determination of the residual opening as a function of $\phi(s_i)$ and from equations (5) and (6) the stresses along the fracture opening can be calculated as

$$\sigma_{xx}(t_j) = \frac{\overline{E}}{4N}\sum_{i=1}^{N}\frac{\phi(s_i)}{t_j - s_i}, \tag{34}$$

and

$$\sigma_{yy}(t_j) = \frac{\overline{E}}{4N}\sum_{i=1}^{N}\frac{\phi(s_i)}{t_j - s_i} + \sigma^{\infty}. \tag{35}$$

The out-of-plane stress component $\sigma_{zz}(t_j)$ can be found from Eq. (7).

Furthermore, the residual opening together with compressive stresses along the fracture can be used to find the permeability of the fracture channel as well as the increase in production rate of a wellbore. Moreover, an indication of the initiation of a local fracture or secondary fracturing, which can significantly affect the production rate [49], may come from the known stress state along the fracture length. As the current paper goal is, however, the development of a computational approach, these interesting and important problems are beyond the scope of the current study.

5 Results and Discussion

5.1 Validation of the proposed method

A similar problem of residual opening was considered earlier with relation to composite patching repair, which is widely used in aircraft industry to restore the strength of damaged structures. Therefore, we perform in this chapter a validation of the developed method against results obtained in these previous studies.

Cox and Rose [50] work focused on the modelling of the non-linear behaviour of composite patching repair to arrest or slow down the growth of a fatigue crack. Despite having a different nature, the mechanical model of composite patching repair has a very similar mathematical formulation to the problem under consideration. The results presented by these authors were adopted as a benchmark for comparison and validation of the mathematical model described in Section 3 and numerical solution method. The work by Cox and Rose [50] utilises elastic/perfectly-plastic springs to model the crack bridging patch. The geometry of the problem addressed by these authors is illustrated in Figure 3. The formulation of the composite patch problem can be reduced to the following system of boundary conditions:

$$\sigma_{yy}(x,y) = \sigma^{\infty} - \sigma'_n(x),\ b \le |x| \le a\,,\ y = 0\,; \tag{36a}$$

$$\sigma'_n(x) = \overline{E}k\delta(x),\ \delta(x) < \delta_p\,; \tag{36b}$$

$$\sigma'_n(x) = \sigma_p = \overline{E}k\delta_p\,; \tag{36c}$$

where k denotes a constant characterising the spring stiffness in the linear range, σ_p is the yield stress, and δ_p is a characteristic crack opening beyond which the spring response changes from being elastic to being perfectly plastic. Additionally, the initial stress intensity factor K_0 and the initial crack opening δ_0 are both zero. The above formulation is much simpler than that for the residual closure of a fracture filled with proppant considered in the current work.

The approach presented by Cox and Rose [50] for the stress intensity factor K and the crack opening $\delta(x)$ is based on a numerical solution of a system of non-linear equations incorporating Eq. (36) and two other relationships well known from fracture mechanics textbooks:

$$K = \sigma^{\infty}\sqrt{\pi a} - \frac{2}{\pi}\sqrt{\pi a}\int_b^a \frac{\sigma'_n(x)}{\sqrt{a^2 - x^2}}dx\,, \tag{37}$$

and

$$\delta(x) = \frac{4\sigma^{\infty}}{\overline{E}}\sqrt{a^2 - x^2} - \frac{4}{\pi\overline{E}}\int_b^a \ln\left|\frac{\sqrt{a^2-\xi^2} + \sqrt{a^2 - x^2}}{\sqrt{a^2-\xi^2} - \sqrt{a^2 - x^2}}\right|\sigma'_n(\xi)d\xi\,. \tag{38}$$

This system can be rewritten in a numerical fashion and solved computationally by means of a self-consistent numerical procedure.

A concise description of the results can be achieved by the adoption of the following normalisations:

$$A = 4ka/\pi \,, \tag{39a}$$

$$B = 4kb/\pi \,, \tag{39b}$$

and

$$K_N = K\sqrt{k}/\sigma_p \,; \tag{39c}$$

with A being the normalised crack length, B the normalised notch length and K_N the normalised stress intensity factor.

The magnitude of the normalised stress intensity factor K_N for various normalised fracture lengths A as predicted by the developed method, for a varying number of integration points, N, is compared against Cox and Rose [50] approach (Eqs. (37) and (38)). This comparison is presented in Figure 4. This figure demonstrates that there is an excellent agreement between the current method and equations presented by Cox and Rose [50] if a sufficient number of integration points, N, is utilised in the numerical solution. Moreover, the convergence of the solution with an increase in the number of integration points is illustrated in Figure 5.

5.2 Stress Intensity Factor

The stress intensity factor for a crack filled with compressible particles has to be bounded by two critical values. The first one is the value of the stress intensity factor, K_0. It corresponds to the fracture which is fully filled $(b = a)$ with incompressible particles. The second limiting value is zero and this corresponds to the opposite case: when the fracture is filled with highly compressive particles or when b tends to zero. The formulation presented earlier (Sections 2 to 4) fully comply with these physical limitations, as it can be seen from the results presented below.

In the following we introduce a new normalised stress intensity factor, K_N^* and a normalised stress, P, which are given by

$$K_N^* = K/K_0 \tag{40a}$$

and by

$$P = C\frac{\sigma'_n - \sigma^\infty}{p + \sigma^\infty}, \tag{40b}$$

respectively.

A full agreement to the above limitations can be found from Figure 6. Figure 6a shows that K is approaching K_0, i.e. $K_N^* \to 1$, for situations where the fracture is fully filled with slightly compressive particles $(C < 0.1)$. On the other hand, Figure 6a verifies that the presence of highly compressible particles $(C > 0.2)$ forces K to zero, i.e. $K_N^* \to 0$. Additionally, an assessment of the effect of the reduction of the settled proppant length is provided by three curves in Figure 6 corresponding to three different lengths. It is obvious that K, once again, tends to zero when the settled proppant length, b, is approaching zero, i.e. $b/a \to 0$.

From Figure 6 one can see the changes in the compressive behaviour of the particle assembly due to variations in the initial effective stress, σ'_{n0}. This parameter describing the mechanical behaviour of the proppant along with the proppant compressibility index, Eq. (12), provide the combined effect of the proppant mechanical properties on the residual fracture opening and, consequently, on the well productivity.

5.3 Fracture Profiles

When assessing the efficiency of a stimulation procedure it is of paramount importance to have an accurate prediction of the fracture residual opening because of the direct connection between the residual opening and the permeability of the fracture channel. From the approach derived above (Sections 2 to 4) it is possible to describe the fracture profiles of hydraulic fractures either fully or partially filled with proppants.

Figure 7 shows the normalised fracture face displacement U (crack opening displacement),

$$U = \frac{\overline{E}}{4a(\sigma^\infty + p)}\delta(x), \tag{41}$$

against the normalised position along the fracture, t – see Eq. (16b). Several b/a ratios were considered, demonstrating the effect of the settled proppant length on the fracture residual opening profile.

From Figure 7 it is possible to draw a few conclusions regarding the influence of the settled proppant on the residual fracture openings. When $b/a = 1$ (or fracture is fully filled with proppant) the maximum possible fracture residual opening profile can be achieved.

When the fracture is partially filled with proppant, or $0 < b/a < 1$, the residual openings experience an abrupt drop at $x = b$ due to the lack of the reaction support provided by the proppant inside the fracture. The stresses along the fracture are redistributed causing the reduction in the maximum opening at the centre of the crack. Finally, in the case of $b/a = 0$, the residual opening tends to zero. This corresponds to the case of full closure after the hydraulic fracture is fully removed in the absence of proppant. However, with the presence of deviatoric stresses in rock formations the full closure of the fracture channels may be prevented by other fracture opening mechanisms, such as, for example, the shear slip opening mechanism [19]. Further, the calculated opening profiles can be utilised to evaluate the permeability of the fracture channel and estimate the increase of the productivity.

6 Conclusions

Despite the success of stimulation procedures targeted to improve well productivity being significantly influenced by the residual opening of fluid driven fractures, only a few authors have addressed this very important problem. This study made an effort aimed to fulfil this gap. A new 2D mathematical model based on the Distributed Dislocation Technique is first developed and presented along with an effective solution method for calculating the residual openings of fractures fully or partially filled with proppant. In this mathematical model there are no limitations on the use of any other particular approach to describe the mechanical response of the proppant to compressive loading. Due to its simplicity and efficiency, the Karl Terzaghi's classical consolidation model was utilised to analyse the effect of both the mechanical properties of the proppant and its distribution inside the fracture on the residual openings.

It was found that the mathematical formulation of the model for composite patching repair of fatigue cracks in the aerospace industry [50] bears some similarities to the problem being considered in this work. These similarities allowed a proper validation of the results obtained by the method employed to solve a system of non-linear system of integral equations. The present method was found to be in an excellent agreement with the previous works as well as the expected physical behaviour for the limiting situations. Furthermore, it was shown that the proppant properties and distribution strongly influence the fracture residual opening profile.

The method for calculating the residual openings can be employed to estimate the increase in the production rate of hydraulically stimulated reservoirs, whereas the calculated stress field provides a means of investigating other important phenomena that can influence the well productivity, such as the secondary cracking.

Acknowledgments

The authors gratefully acknowledge the support provided by the Australian Research Council via research grants DP1094299 and LP100100613.

References

[1] Warpinski NR, Moschovidis ZA, Parker CD, Abou-Sayed IS. Comparison Study of Hydraulic Fracturing Models—Test Case: GRI Staged Field Experiment No. 3. SPE Prod. Facil. 1994;9:7–16.

[2] Mahrer KD. A review and perspective on far-field hydraulic fracture geometry studies. J. Pet. Sci. Eng. 1999;24:13–28.

[3] Economides MJ, Nolte KG. Reservoir Stimulation. 3rd ed. Chichester: Wiley; 2000.

[4] Rahman MM, Rahman MK. A Review of Hydraulic Fracture Models and Development of an Improved Pseudo-3D Model for Stimulating Tight Oil/Gas Sand. Energ. Source Part A 2010;32:1416–36.

[5] Vincent MC. Proving It - A Review of 80 Published Field Studies Demonstrating the Importance of Increased Fracture Conductivity. In: Proceedings of the SPE Annual Technical Conference and Exhibition. San Antonio, Texas; 29 September – 2 October 2002. p. 21.

[6] Kern LR, Perkins TK, Wyant RE. The Mechanics of Sand Movement in Fracturing. J. Petrol. Technol. 1959;11:55–7.

[7] Wahl H, Campbell J. Sand Movement in Horizontal Fractures. J. Petrol. Technol. 1963;15:1239–46.

[8] McLennan JD, Green SJ, Bai M. Proppant Placement During Tight Gas Shale Stimulation: Literature Review And Speculation. In: Proceedings of the 42nd U.S. Rock Mechanics Symposium. San Francisco, California; 29 June – 2 July 2008. p. 14.

[9] Clark PE, Güler N. Prop Transport in Vertical Fractures: Settling Velocity Correlations. In: Proceedings of the SPE/DOE Low Permeability Gas Reservoirs Symposium. Denver, Colorado; 14–16 March 1983. p. 6.

[10] Daneshy AA. Numerical Solution of Sand Transport in Hydraulic Fracturing. In: Proceedings of the SPE 50th Annual Fall Meeting. Dallas, Texas; 28 September 28 – 1 October 1975.

[11] Daneshy AA. Numerical Solution of Sand Transport in Hydraulic Fracturing. J. Petrol. Technol. 1978;30:132–40.

[12] Novotny EJ. Proppant Transport. In: Proceedings of the SPE Annual Fall Technical Conference and Exhibition, Denver, Colorado; 9–12 October 1977. p. 12.

[13] Clifton RJ, Wang J-J. Multiple Fluids, Proppant Transport, and Thermal Effects in Three-Dimensional Simulation of Hydraulic Fracturing. In: Proceedings of the SPE Annual Technical Conference and Exhibition. Houston, Texas; 2–5 October 1988. p. 14.

[14] Unwin AT, Hammond PS. Computer Simulations of Proppant Transport in a Hydraulic Fracture. In: Proceedings of the SPE Western Regional Meeting. Bakersfield, California; 8–10 March 1995. p. 16.

[15] Smith MB, Klein HH. Practical Applications of Coupling Fully Numerical 2-D Transport Calculation with a PC-Based Fracture Geometry Simulator. In: Proceedings of the SPE Annual Technical Conference and Exhibition. Dallas, Texas; 22–25 October 1995. SPE 30505.

[16] Gadde P, Yajun L, Jay N, Roger B, Sharma M. Modeling Proppant Settling in Water-Fracs. In: Proceedings of the SPE Annual Technical Conference and Exhibition. Houston, Texas: SPE 89875-MS; 26–29 September 2004. p. 10.

[17] Poe Jr. BD, Economides MJ. Chapter 12: Post-Treatment Evaluation and Fractured Well Performance. In: Reservoir Stimulation, MJ Economides, KG Nolte, editors. Chichester: Wiley; 2000. p. 41.

[18] Dyskin AV, Galybin AN. Solutions for dilating shear cracks in elastic plane. Int. J. Fract. 2001;109:325–44.

[19] Ghassemi A, Tarasovs S, Cheng AH-D. A 3-D study of the effects of thermomechanical loads on fracture slip in enhanced geothermal reservoirs. Int. J. Rock Mech. Min. Sci. 2007;44:1132–48.

[20] Kotousov A, Bortolan Neto L, Rahman SS. Theoretical model for roughness induced opening of cracks subjected to compression and shear loading. Int. J. Fract. 2011;172:9–18.

[21] Kotousov A, Codrington JD. Chapter 5: Application of Refined Plate Theory to Fracture and Fatigue. In: Structural Failure Analysis and Prediction Methods for Aerospace Vehicles and Structures, SY Ho, editor. Sharjah, UAE: Bentham Science Publishers; 2010. pp. 90–103.

[22] Hills DA, Kelly PA, Dai DN, Korsunsky AM. Solution of crack problems: the distributed dislocation technique. London: Kluwer Academic Publishers; 1996.

[23] Terzaghi K, Peck RB, Mesri G. Soil mechanics in engineering practice. 3rd ed. New York: John Wiley & Sons; 1996.

[24] Bortolan Neto L, Kotousov A, Bedrikovetsky P. Application of Contact Theory to Evaluation of Elastic Properties of Low Consolidated Porous Media. Int. J. Fract. 2011;168:267–76.

[25] Bortolan Neto L, Kotousov A, Bedrikovetsky P. Elastic properties of porous media in the vicinity of the percolation limit. J. Pet. Sci. Eng. 2011;78:328–33.

[26] Adachi J, Siebrits E, Peirce A, Desroches J. Computer simulation of hydraulic fractures. Int. J. Rock Mech. Min. Sci. 2007;44:739–57.

[27] Batchelor GK. An Introduction to Fluid Dynamics. Cambridge: Cambridge University Press; 2000.

[28] Adachi JI, Detournay E, Peirce AP. Analysis of the classical pseudo-3D model for hydraulic fracture with equilibrium height growth across stress barriers. Int. J. Rock Mech. Min. Sci. 2010;47:625–39.

[29] Chekhonin E, Levonyan K. Hydraulic fracture propagation in highly permeable formations, with applications to tip screenout. Int. J. Rock Mech. Min. Sci. 2012;50:19–28.

[30] Desroches J, Detournay E, Lenoach B, Papanastasiou P, Pearson JRA, Thiercelin M, Cheng A. The Crack Tip Region in Hydraulic Fracturing. Proc. R. Soc. Lond. A 1994;447:39–48.

[31] Atkinson C, Thiercelin M. The interaction between the wellbore and pressure-induced fractures. Int. J. Fract. 1993;59:23–40.

[32] Mogilevskaya SG, Rothenburg L, Dusseault MB. Growth of Pressure-Induced Fractures in the Vicinity of a Wellbore. Int. J. Fract. 2000;104:23–30.

[33] Zhang X, Jeffrey RG, Bunger AP, Thiercelin M. Initiation and growth of a hydraulic fracture from a circular wellbore. Int. J. Rock Mech. Min. Sci. 2011;48:984–95.

[34] Lin'kov AM, Mogilevskaya SG. Hypersingular integrals in plane problems of the theory of elasticity. J. Appl. Math. Mech. 1990;54:93–9.

[35] Linkov AM, Mogilevskaya SG. Complex hypersingular integrals and integral equations in plane elasticity. Acta Mech. 1994;105:189–205.

[36] Mogilevskaya SG. Complex hypersingular integral equation for the piece-wise homogeneous half-plane with cracks. Int. J. Fract. 2000;102:177–204.

[37] Chan Y-S, Fannjiang AC, Paulino GH. Integral equations with hypersingular kernels—theory and applications to fracture mechanics. Int. J. Eng. Sci. 2003;41:683–720.

[38] Cruse TA. BIE fracture mechanics analysis: 25 years of developments. Comput. Mech. 1996;18:1–11.

[39] Aliabadi MH. A new generation of boundary element methods in fracture mechanics. Int. J. Fract. 1997;86:91–125.

[40] Bilby B, Eshelby J. Chapter 2: Dislocations and the theory of fracture. In: Fracture: An Advanced Treatise vol. 1, H Liebowitz, editor. New York: Academic Press; 1968. pp. 99–182.

[41] Kotousov A. Fracture in plates of finite thickness. Int. J. Solids Struct. 2007;44:8259–73.

[42] Pestana JM, Whittle AJ. Compression model for cohesionless soils. Geotechnique 1995;45:611–31.

[43] Vesic AS, Clough GW. Behavior of granular materials under high stresses. Proc. ASCE: J. Soil Mech. Found. Div. 1968;94:661–88.

[44] Coduto DP. Foundation design: principles and practices. Upper Saddle River, New Jersey: Prentice Hall; 2001.

[45] Codrington J, Kotousov A. Application of the distributed dislocation technique for calculating cyclic crack tip plasticity effects. Fatigue Fract. Eng. Mater. Struct. 2007;30:1182–93.

[46] Codrington J, Kotousov A. The distributed dislocation technique for calculating plasticity-induced crack closure in plates of finite thickness. Int. J. Fract. 2007;144:285–95.

[47] Rheinboldt WC. Methods for Solving Systems of Nonlinear Equations. 2nd ed. Philadelphia: SIAM; 1998.

[48] Bathe K-J. Finite element procedures. Upper Saddle River, New Jersey: Prentice Hall; 1996.

[49] Aghighi MA, Rahman SS. Initiation of a secondary hydraulic fracture and its interaction with the primary fracture. Int. J. Rock Mech. Min. Sci. 2010;47:714–22.

[50] Cox BN, Rose LRF. A self-consistent approximation for crack bridging by elastic/perfectly plastic ligaments. Mech. Mater. 1996;22:249–63.

Table 1. Classification of the particle assembly compressibility [44]

Compressibility, C	Classification
0 – 0.05	Very slightly compressible
0.05 – 0.10	Slightly compressible
0.10 – 0.20	Moderately compressible
0.20 – 0.35	Highly compressible
> 0.35	Very highly compressible

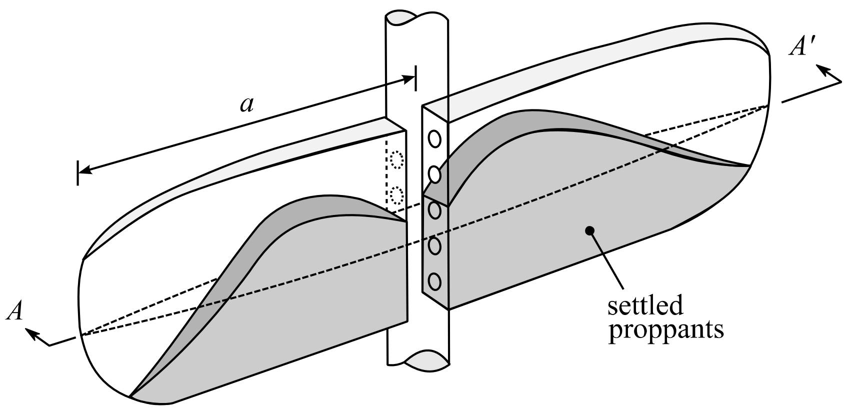

Figure 1. Proppant build up in a hydraulic fracture. The cross section AA' is depicted in detail in Figure 2a (not to scale).

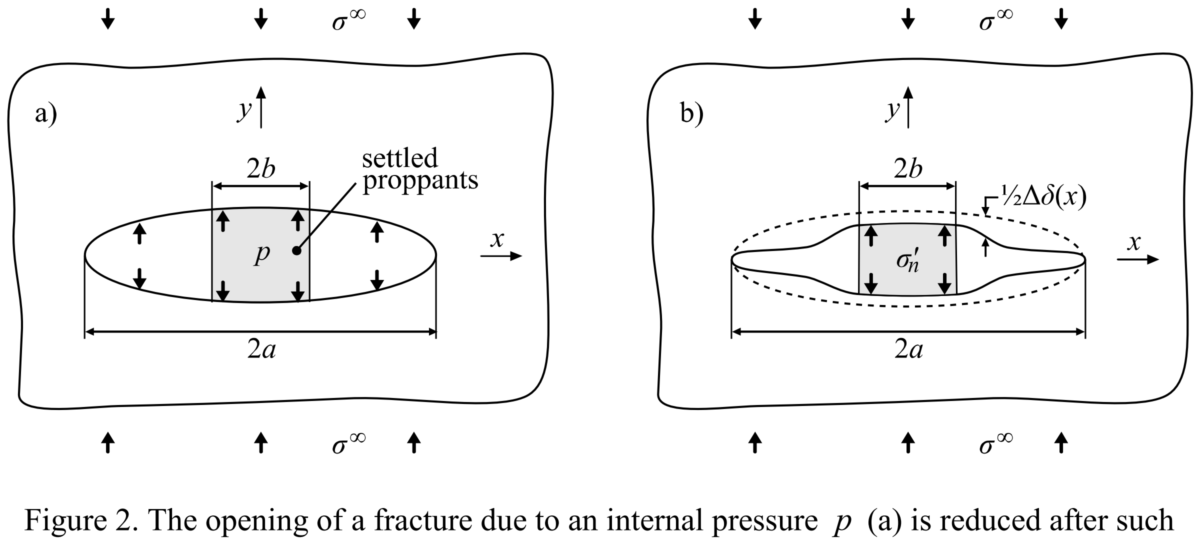

Figure 2. The opening of a fracture due to an internal pressure p (a) is reduced after such pressure is removed (b). The full closure of the fracture is prevented by the normal stress due to proppant, σ_n'.

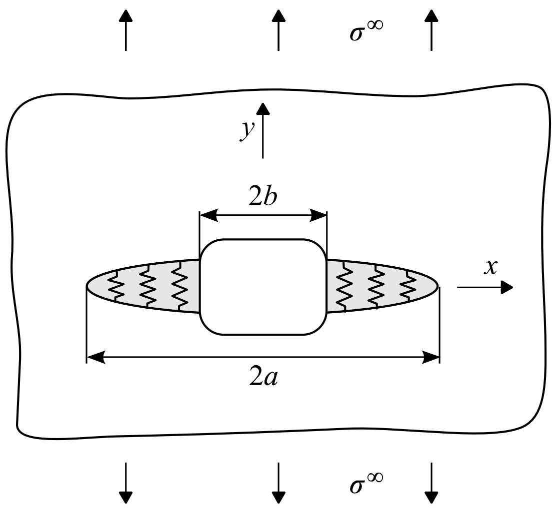

Figure 3. The geometry of the composite patching repair of fractures problem.

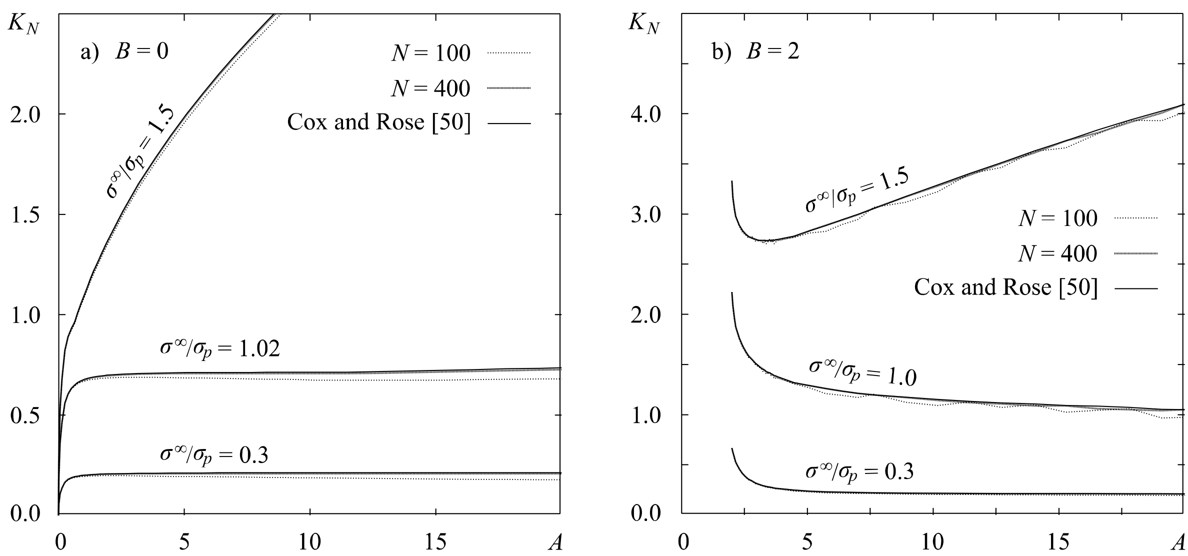

Figure 4. Normalised stress intensity factor K_N development for both elastic and elastic/perfectly-plastic cases. Situations (a) with zero notch length $(B = 0)$ and (b) with moderate notch length $(B = 2)$ are shown.

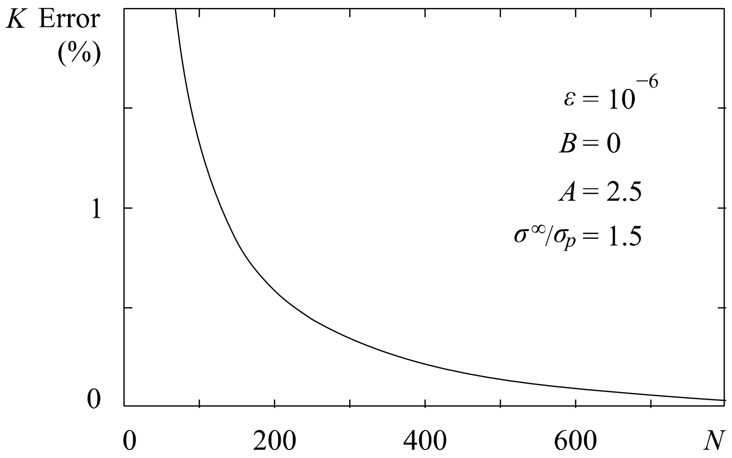

Figure 5. Stress intensity factor error versus the number of integration points.

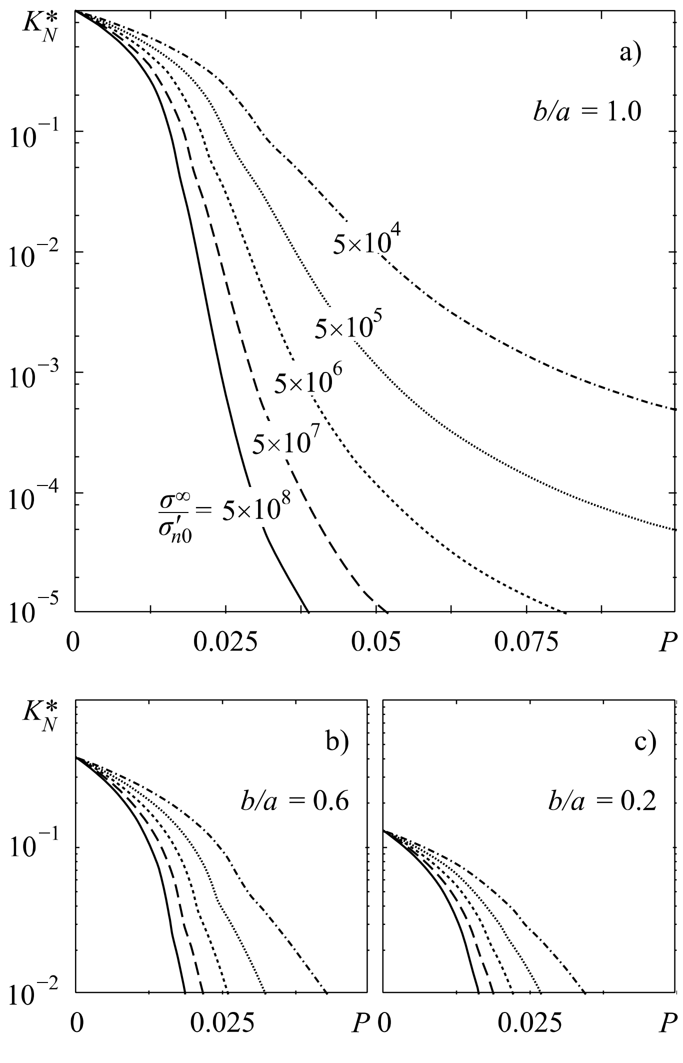

Figure 6. Normalised stress intensity factor K_N^* versus the normalised stress P as a function of various $\sigma^{\infty}/\sigma'_{n0}$ ratios. Both fully filled (a) and partially filled (b and c) fracture opening cases were considered.

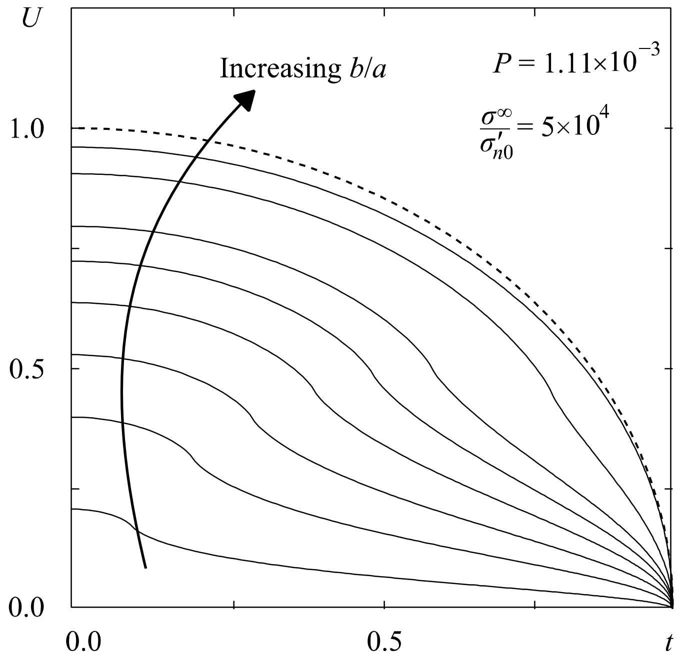

Figure 7. Normalised residual fracture profiles for a variety of b/a ratios. The dashed curve represents the normalised fracture initial opening. When $b/a = 0$, $U(t) = 0$.